

Exosomal Moesin Derives From Ectopic Stromal Cells Constructs A “Migration-Vascularization-Inflammation” Loop In Endometriosis

Maidinaimu Abudula

Ningbo University Medical School

Xiaodan Fan

Ningbo University Medical School

Jing Zhang

Affiliated Hospital of Medical School Ningbo University and Ningbo City Third Hospital

Jiajie Li

Affiliated Hospital of Medical School Ningbo University and Ningbo City Third Hospital

Xiaoming Zhou

Affiliated Hospital of Medical School Ningbo University and Ningbo City Third Hospital

Yichen Chen (✉ cyc_0605@hotmail.com)

Ningbo Institute of Medical Science <https://orcid.org/0000-0001-5726-9383>

Research Article

Keywords: Exosomal Moesin, Endometriosis, Migration, Vascularization, Inflammation

Posted Date: June 29th, 2021

DOI: <https://doi.org/10.21203/rs.3.rs-616514/v1>

License: © ⓘ This work is licensed under a Creative Commons Attribution 4.0 International License.

[Read Full License](#)

Abstract

Background: Endometriosis (EMS) is the most common gynaecological disorder with its etiology and/or pathophysiology remains enigmatic. Recent studies showed that extracellular vesicles (EVs), exosomes namely, play a critical role in the development of various clinical disorders, including inflammatory disease and cancers. Previous studies revealed the role of exosomes as a potential biomarker in EMS. However, the implication of exosomes in the disease progression of EMS has not been well elucidated.

Method: The biological function of ectopic exosomes (eEVs) was examined by Transwell assay, scratch tests, tube formation assay, western blot, and qRT-PCR analysis. Mass spectrometry analysis of the exosomes isolated from fresh EMS tissue and vaginal discharge obtained from patients with and without EMS used to identify differentially expressed protein in exosomes from ectopic stromal cells (ESCs) and normal endometrial stromal cells (NESC). Gene knockdown was used to downregulate the expression of exosomal protein in *in-vivo* setting. Finally, *in-vitro* experiment confirmed the results that we observed in endometriosis (EMS) mouse model.

Results: We found that eEVs increased the migration ability of NESC) by up-regulating MMP9 expression. We also observed that eEVs facilitate angiogenesis, and induced the high expression of inflammatory cytokines in ovarian epithelial cells. Protein Mass spectrometry and bioinformatics analysis showed that Moesin (MSN) is highly expressed in eEVs. An abnormal high estrogen environment may up-regulate MSN expression in ectopic lesion. Downregulation of exosomal Moesin attenuated the migration capability of normal endometrium, inhibited angiogenesis, and reduced the expression of inflammatory cytokine. Moreover, we found that ectopic exosomes significantly increased the number and size of heterotopic foci *in vivo*. Also, we observed an increase in the size of vascular lumen, and upregulation of inflammatory factors expression in small intestine adjacent to the heterotopic foci.

Conclusion: Exosomal MSN from ectopic stromal cells could contribute to the development of EMS by mediating the construction of a “migration-vascularization-inflammation” loop in ectopic environment.

Introduction

Endometriosis (EMS) is a chronic and inflammatory gynaecological condition characterized by the implantation and growth of endometrial-like tissue outside the uterus cavity [1]. EMS affects up to 10% of women of reproductive age, accompanied by chronic pelvic pain, irregular menstruation, and infertility in as many 50% of affected women [2]. Although many theories have been proposed to explain the onset of endometriotic lesions, the etiopathology of this disease remains unknown. Amongst the proposed theories, Sampson's theory of retrograde menstruation is the most accepted one worldwide. Sampson's theory proposed that endometriosis is caused due to the retrograde flow of endometrial cells/debris through the fallopian tube into the peritoneal cavity during menstruation. Admittedly, approximately 80 to 90 % of women undergo retrograde menstruation; however, only around 5–10% of women develop EMS [3, 4]. This notable difference between the two proportions indicates that the refluxed endometrial tissue

is not the only cause for the development of endometriosis. There may be additional responses to the ectopic endometrium in the local environment that enables their implantation and further development into endometriotic lesions. In addition, increasing evidence indicates that the successful establishment and survival of ectopic implants in the ectopic microenvironment (peritoneal cavity or pelvic organs) require tumor-like migration and invasion, adhesion formation, vascularization, fibrosis, and neuronal infiltration [5] [6] [7].

Inflammation and angiogenesis at the site of the ectopic implant have been considered to involve in the development of endometriotic lesions [8] [9]. Previous studies reported the high concentration of pro-inflammatory cytokines in the peritoneal fluid of endometrial patients [8]. Recent in-vitro studies have also shown that endometriotic lesion possesses the ability to produce endometriosis-related cytokines and/or regulators of cytokine production to facilitate systemic inflammation, as well as stimulating angiogenesis [10] [11]. However, whether the observed high concentration of cytokines and peritoneal fluid is the cause or the consequences of EMS has yet to be further described. More importantly, it is still unclear which factors are regulating the inflammation and angiogenesis at the site of ectopic implantation caused by retrograde endometrium.

Exosomes have been emerged as an important regulator of cell-cell communication within the surrounding microenvironment, with their critical feature as a natural carrier of biological information including nucleic acids, proteins, and lipids [12] [13]. Tumor-derived exosomes have been shown to contribute to the progression and metastasis of cancer by transferring genetic molecules from their parent cells to recipient cells, thereby regulating the biological function of recipient cells [14] [15]. Recent studies on exosomes' implications in the development of endometriosis, particularly in the ectopic microenvironment, have improved our understanding of endometriosis. The best example is that, in endometriosis, exosomes carrying certain gene molecules, such as miRNA and/or lncRNAs which are implicated in inflammation, fibrosis, and angiogenesis, have been shown to involve in the development of EMS [16] [17] [18]. However, the involvement of the exosomal protein in the establishment of endometrial lesions, and the pathophysiology of EMS have not been well characterized.

In this study, we observed that exosomes isolated from ectopic endometrial cells induce the migration and angiogenesis in healthy endometrial cells, and also stimulate the production of inflammatory cytokines in ovarian epithelial cells. It is therefore hypothesized that the primary ectopic endometrial lesions may target the upcoming eutopic endometrium of reflux, as well as the surrounding microenvironment by releasing exosomal protein, therefore establishing an ectopic microenvironment with a property of "migration-inflammation-angiogenesis" loop that suitable for the development of endometriotic lesions.

Materials And Methods

Patients and Samples

All the clinical specimens including, endometrial tissue and vaginal secretion (leukorrhea), were collected from the patients who enrolled in the Affiliated Hospital of Ningbo Medical School of Ningbo University (Ningbo, China)(The general condition of patients in **table 1**. The primary normal endometrium samples were collected from the reproductive-age women undergoing surgery for other benign gynaecological conditions (n = 10). Primary ectopic endometrial stromal cells were obtained from women with endometriosis, ovarian endometriosis, particularly (n = 6). The vaginal secretion (leukorrhea) was collected from corresponding endometriosis patients. For the control group, vaginal secretion specimens were obtained from patients without endometriosis and any other hormone-related disorders, and women with the normal menstrual cycle were admitted for physical examination. Ovarian epithelial cells were isolated from the ovarian tissue obtained from patients who underwent bilateral appendices hysterectomy excluded from endometriosis. All the subjects selected were women free from hormonal therapy for three months and had regular menstrual cycles. Samples obtained from all patients and controls were matched for the secretory phase of the menstrual cycle. Written informed consent was obtained from all women before the sample collection, and all procedures were approved by the ethical committee of the Affiliated Hospital of Ningbo Medical School of Ningbo University (Ningbo, China).

Table 1. The general condition of patients

Sample Number	Gender	Age (y)	Pathological Diagnosis	Menstrual Cycle (Days)	Ectopic Tissue Size (mm)	Dysmenorrhea (Y/N)	CA125 (U/ml)
1	F	34	Ovaria Chocolate cyst	5/30	58	N	64
2	F	27	Ovaria Chocolate cyst	5/30	72	Y	40
3	F	33	Ovaria Chocolate cyst	5/29	64	N	49
4	F	30	Ovaria Chocolate cyst	6/31	55	Y	51
5	F	32	Ovaria Chocolate cyst	5/30	61	N	45
6	F	33	Ovaria Chocolate cyst	5/30	57	N	47
7	F	27	Abortion	6/30	-	N	-
8	F	38	Myoma of uterus	5/29	-	Y	45
9	F	29	Myoma of uterus	6/31	-	N	51
10	F	37	Myoma of uterus	5/30	-	N	55
11	F	38	Myoma of uterus	5/29	-	N	69
12	F	32	Myoma of uterus	5/30	-	Y	46
13	F	29	Abortion	5/29	-	N	-
14	F	30	Abortion	6/31	-	N	-
15	F	35	Myoma of uterus	6/30	-	N	75
16	F	36	Myoma of uterus	6/29	-	N	55

Cell Culture

Primary normal endometrial stromal cells (NESC), ectopic endometrial stromal cells (ESC) were isolated from endometrial tissue after tissue digestion. Digested tissue was filtered through 100µm and 40 µm mesh to collect the stromal cells. Cells were then incubated in DME/F12 medium (Gibco, USA) supplemented with 10% fetal bovine serum (FBS) (Gibco, USA), 1 % penicillin (100 U/mL) and streptomycin (100 µg/mL) at 37°C and 5 % CO₂ in a humidified incubator. Human umbilical vein endothelial cells (HUVECs) were purchased from the cell bank of the Chinese Academy of Sciences (China) and were cultured in DMEM complete medium. Ovarian epithelial cells were cultured in DME/F12 medium supplemented with 10% FBS and 1% penicillin and streptomycin. All of the primary cells were cultured less than 14 days in vitro environment, and only passage 1 (P1) cells were taken for subsequent experiments.

Exosomes isolation and identification

Exosomes were isolated from NSCs and ESCs culture supernatant, as well as patients' vaginal secretion. NSCs and ESCs were incubated primarily in culture media with 10% exosomes-free FBS, which was obtained by 12h ultracentrifugation of FBS at 100,000g at 4°C. After 48h of incubation, cell culture supernatants were collected, and exosomes were isolated as previously described[19]. Subsequently, exosomal protein concentrations were determined using bicinchoninic acid (BCA) protein assay kit (Thermo Scientific, USA) according to the manufacturer's instructions. All exosomal protein samples were standardized to the quantity of 10ug for in-Vitro and 20µg for the in-Vivo experiment. Then, exosomal classical marker CD9, CD63, and CD81 (Cell Signalling Technology, Beverly, MA, USA) expression was measured using western blot analysis. The aliquots were stored at - 80°C for subsequent experiments. The extracted exosomes and pellets were sent to Hibio Technology Co., Ltd. (Hangzhou, China) for transmission electron microscope (TEM) observation and validation, and the size distribution measurement analysis.

Fluorescent labeling of exosomes

This assay was performed to identify the internalization of the exosomes from ESCs into NSCs. Briefly, isolated exosomes were re-suspended in 500 µl of PBS in a 1.5 ml microcentrifuge tube (Eppendorf, EP), and DiR (1,1'-dioctadecyl-3,3,3',3'-tetramethylindotricarbocyanine iodide, Dalian Meilun Biotechnology Co. Ltd., China) with a final concentration of 5 µg/ml was added to label the exosomes and incubated at 37°C for 30 min without shaking. Labeled exosomes were centrifuged at 10000×g for 10 min, and the supernatant was carefully filtered with a 0.22-µm filter. DiR-labeled exosomes were then co-cultured with NSCs for 24 h in a 6-well plate. The cells were then prepared for immunofluorescence analysis, and the internalization of exosomes was subsequently observed under a fluorescence microscope.

Migration and wound-healing assay

Cells were pre-treated with exosomes (5µg/ml) or with exosomes-free culture medium for 24h. For the migration assay, approximately 4×10^4 cells were seeded into the upper transwell chambers and incubated with an FBS-free culture medium, while the lower chambers were maintained in a culture medium with 10% FBS. After 24h incubation, all cells transferred to the lower chambers were fixed with 2% methanol and stained with 0.5% crystal Violet. Positive staining cells from six representative fields of

chambers in each group were photographed and counted under a microscope (CKX40, Olympus, Japan). For wound healing assays, cells were pre-treated with exosomes and exosomes-free culture medium as previously described, equal amounts of cells were plated into six-well plates. Cells monolayer were scratched with a pipette tip to draw a gap between cells on the bottom of the plates, cell migration was observed, and images were taken at 0h, 24h, and 48h time point. Subsequently, the number of migrating cells was quantified using Image-pro plus (PPI, USA)

Matrigel tube formation assay

HUVEC were pre-treated with both NSCs, and ESCs derived exosomes (5µg/ml) or with PBS as a control for 24h. About 2.5×10^4 HUVEC cells were seeded in growth factor-reduced Geltrex Basement Membrane Matrix (BD, USA) on a 96-well plate and incubated up to 2h at 37°C with 5% CO₂. The formation of the tube was observed under the microscope, and images were captured. Formative tube length was determined using Image J software. Results are presented as the mean and standard errors.

Western Blotting

The total proteins of cells and exosome pellets were lysed with RIPA buffer supplemented with proteinase inhibitors (Beyotime Biotechnology, China), as per manufacturer's protocols, and centrifuged at 14,000×g for 10 min at 4°C. Protein concentrations were determined using the BCA protein assay kit, as previously described. Protein samples were (25µg if extracted from cells and 35µg if extracted from exosomes) separated by 8%-12% sodium dodecyl sulfate-polyacrylamide gel electrophoresis (SDS-PAGE), and transferred onto 0.22µm polyvinylidene difluoride (PVDF) membranes. Membranes were blocked in 5% skim milk TBS-T solution for one hour at room temperature and incubated with primary antibody overnight at 4°C. The following primary antibodies were used in this blotting: anti-CD9 (1:1000; CST, USA), anti-CD63 (1:1000; CST, USA), anti-CD81 (1:1000; CST, USA), anti-GAPDH (1:3000; Bios, China), anti-VEGFR (1:1000; CST, USA), anti-pVEGFR2 (1:1000; CST, USA), anti-PDGFR (1:1000; CST, USA), anti-pPDGFR (1:1000; CST, USA), anti-ERα (1:1000, Abcam, USA), anti-Gα₁₃ (1:200, Santa-Cruz, USA), anti-RhoA (1:200, Santa-Cruz, USA), anti-ROCK-2 (1:200, Santa-Cruz, USA), anti-MSN (1:500, Proteintech, China), anti-MMP9 (1:1000, Absin, China), anti-MSN (1:500, Absin, China), Epithelial-Mesenchymal Transition (EMT) Antibody Sampler Kit (#9782, CST, USA), anti-Moesin (1:1000, Absin, China) followed by incubation with appropriate horseradish peroxidase-conjugated secondary antibodies at room temperature for 2 hours. Subsequently, immune-reactive protein bands were visualized with chemiluminescence reagents (CST, USA), followed by imaging on an electrophoresis gel imaging analysis system (GENE, USA).

RNA extraction and quantitative real-time polymerase chain reaction (qRT-PCR)

Total RNA was extracted from cultured cells and purified exosomes using TRIzol™ reagent (Life Technologies, USA), following the manufacturer's instructions. The extracted RNA was re-suspended in 20–30µl RNase-free DEPC water and stored at –80°C. 500ng of total RNA was used for qRT-PCR analysis. The cDNA was synthesized using a transcription kit as per the manufacturer's instructions (CWBio, Beijing, China). The qRT-PCR analysis was conducted using the SYBR Green PCR Kit (CWBio, Beijing, China) on an Applied Biosystems 7500 Real-Time PCR System and associated software (Applied Biosystems, USA). After the initial denaturation step at 95° C for 10mins, three-step amplification was

performed (95° C for 15 s, 60° C for 35 s) for 40 cycles. Relative expression levels of mRNAs were calculated with $2^{-\Delta Ct}$ formula or $2^{-\Delta\Delta Ct}$ using *GAPDH* (glyceraldehyde-3-phosphate dehydrogenase) as an internal control. Specific mRNA primers used for qRT-PCR are presented in **Table 2**.

Table 2: The primer sequence of inflammation cytokines

Primer Name	Sequence 5'-3'
hTNF-a F	CCTCTCTCTAATCAGCCCTCTG
hTNF-a R	GAGGACCTGGGAGTAGATGAG
hIL-1 β F	ATGATGGCTTATTACAGTGGCAA
hIL-1 β R	GTCGGAGATTCGTAGCTGGA
hIL-18 F	TCTTCATTGACCAAGGAAATCGG
hIL-18 R	TCCGGGGTGCATTATCTCTAC
hIFN- α 1 F	GCCTCGCCCTTTGCTTTACT
hIFN- α 1 R	CTGTGGGTCTCAGGGAGATCA
hICAM-1 F	ATGCCCAGACATCTGTGTCC
hICAM-1 R	GGGGTCTCTATGCCCAACAA
mTNF-a F	CCCTCACACTCAGATCATCTTCT
mTNF-a R	GCTACGACGTGGGCTACAG
mIL-1 β F	GCAACTGTTCTGAACTCAACT
mIL-1 β R	ATCTTTTGGGGTCCGTCAACT
mIL-18 F	GACTCTTGCGTCAACTTCAAGG
mIL-18 R	CAGGCTGTCTTTTGTCAACGA
mICAM-1 F	GTGATGCTCAGGTATCCATCCA
mICAM-1 R	CACAGTTCTCAAAGCACAGCG

LC-MS/MS analysis and Bioinformatics analysis

The Whole EVs Lysate from NSCs and ESCs were run for 20 min on a 4–20% SDS-PAGE system to separate proteins from lower molecular weight contaminants. The entire protein region of the gel was excised and subjected to in-gel trypsin digestion after reduction with dithiothreitol and alkylation with iodoacetamide. Peptides eluted from the gel were lyophilized and re-suspended in 25–50 μ l of 5% acetonitrile (0.1% Formica acid) at 4 μ L/min for 4min onto a 100 μ m I.D. Fused-silica pre-column packed with 2cm of 5 μ m nano viper (Thermo, USA). Peptides were eluted at 300 μ L/min from a 75 μ m I.D. gravity-pulled analytical column, packed with 25cm of 3 μ m Magic C18AQ particles using a linear gradient from

5–35% of mobile phase B (acetonitrile + 0.1% formic acid) in mobile phase A (water + 0.1% formic acid) over 60 min. Ions were introduced by positive electrospray ionization via a liquid junction at 1.4–1.6 kV into a Q Exactive hybrid mass spectrometer (Thermo Scientific). Mass spectra were acquired over m/z 300–1750 at 70,000 resolution (m/z 200) with an AGC target of 1×10^6 , and data-dependent acquisition selected the top 10 most abundant precursor ions for tandem mass spectrometry by HCD fragmentation using an isolation width of 1.6 Da, max fill time of 110 ms and AGC target of $1e^5$. Peptides were fragmented by normalized collisional energy of 27, and fragment spectra were acquired at a resolution of 17,500 (m/z 200).

A total of proteins in NESCs and ESCs exosomes were input to FunRich software (3.1.3) for GO (Gene Ontology) enrichment analysis [20]. The gene symbols retrieved from the UniProtKB accession number were mapped to cellular components, molecular function, and biological processes items. The protein comparison between NESCS exosomes and ESCs exosomes using the iBAQ method, the fold change of the protein was calculated by the logarithm of the ratio of individual protein values normalized to the average of the corresponding iBAQ values in the NESCs exosomes ($n = 2$). The significant expression threshold was defined as a criterion of significance value < 0.05 and fold change > 2 ($\log_2 FC > 1$ or < -1). Cytoscape software and the KEGG pathway were used to analyze, integrate, and categorized the data.

Transfection of ESR1 and MSN siRNA in vitro

ESCs were seeded in the 10cm dish at 80% confluency and incubated in a culture medium supplemented with exosomes-free FBS for 24h. ESCs were then transiently transfected with Moesin siRNA (MSNi) 20nM (Genepharma Cop., Shanghai, China) with lipofectamine-2000TM (Invitrogen, USA). After 24h of transfection, the cell culture supernatants were collected for three consecutive days. Exosomes were isolated from ESCs supernatants, and western blot analysis was performed to confirm the expression level of Moesin in exosomes. Then, NSCs were incubated with exosomes^{MSNi} and non-transfected ESCs for 24h and were prepared for subsequent experiments.

ESCs were seeded in the 6-wells plate at 60% confluency and transfected with ESR1 (estrogen receptor 1) siRNA 20nM (Invitrogen, USA) with lipofectamine iMax (Invitrogen, USA). After 48h of transfection, added estrogen (Meilun, Dalian, China) 10nM, 50nM, 100nM into cell culture and collected cell protein after 24h treatment.

Mouse model of Endometriosis

All animal experiments were approved by the committee on the Ethical Use of Animals of Medical School of Ningbo University. Experimental mice were kept following the Guide for the Care and Use of Laboratory animals, in a well-controlled, pathogen-free environment with regulated cycles of light/dark (12h/12h, 23–25°C), and given two weeks of adaptation before any experiments were conducted.

Briefly, 30 female nude mice (Balb/c, 5–6 weeks old), were divided randomly into six subgroups (PBS control, normal endometrium, ectopic endometrium, ectopic endometrium + MSNi, normal endometrium + ESCs-derived exosomes, normal endometrium + ESC-derived exosomal MSNi) before implantation, with

five mice in each group. Prepared cell suspensions for five different groups (about 1×10^7 /ml cells in each suspension) were administrated by peritoneal injection into each mice on day 0. Mice were weighed and recorded every two days. After ten days of observation, mice were then sacrificed and dissected to determine the heterotopic inoculation of endometrial tissue on the intestinal wall.

Immunohistochemistry

Formalin-fixed paraffin-embedded (FFPF) mouse ectopic endometrial tissues were sectioned into $4 \mu\text{m}$ thick tissue slices. Slices were deparaffinized in xylene, rehydrated through graded ethanol, and boiled for 10 min in citrate buffer (10 mM, pH 6.0) for antigen retrieval. Endogenous peroxidase activity was suppressed by exposure to 3% hydrogen peroxide for 10 min. Tissue slides were then blocked with 5% BSA (bovine serum albumin; Boster Bioengineering, Wuhan, China), and incubated overnight at 4°C with the following primary antibodies: anti-MMP9 (Absin, China) and anti-VEGFR2 (CST, USA), followed by incubation with corresponding secondary antibody for 20 min. Slides were visualized, adding DAB (3,3'-diaminobenzidine) substrate, counterstained with hematoxylin, and mounted for observation under the microscope.

Immunofluorescence

Deparaffinization and antigen retrieval was performed as previously described. Tissue sections were then permeabilized by 0.1% TritonX-100 (Sigma Aldrich) for 10 min. Unspecific bindings were blocked by using PBS + 8% Normal goat serum for 1 hour at RT. Tissue sections were incubated overnight at 4°C with the following anti-pVEGFR2 (1:200, CST USA). On the second day, slides were washed 3 times in PBS and incubated with the secondary antibody: Goat anti-rabbit antibody 488 (Abcam, USA) for 1 hour at RT. Finally, sections were mounted using Fluorescent Mounting Medium and visualized under the microscope (Leica Germany).

ELISA detected the expression of Moesin in small extracellular vesicles derived from vaginal secretion

According to the manufacturer's instructions, the small extracellular vesicles collected from vaginal secretion were assayed by Moesin ELISA (Cloud-Clone Corp., China). Exosomes' protein concentrations were uniformly in 10ug to be detected.

Statistical Analysis

The statistical analysis was performed using GraphPad Prism version 6.0 (GraphPad) and SPSS software (version 20.0; IBM Corp., Armonk, NY, USA). Comparisons between two group experiments were performed using a two-tailed Student's t-test, while multiple comparisons between the groups were analyzed using a one-way analysis of variance (ANOVA), followed by the Student Newman-Keuls test. All experiments were performed in triplicate, and the quantification of results was presented as the mean \pm standard deviation. $P < 0.05$ was considered statistically significant.

Results

Identification of exosomes derived from endometrial cells and vaginal discharge

Exosomes were isolated from ESCs incubated for 48 h in exosomes-free culture medium and patients vaginal discharge by ultracentrifugation as previously described. CD9, CD63, and CD81 as recognized exosome-specific markers were used to confirm isolated exosomes using western blot analysis (**Figure. 1a.**). The TEM images showed that the majority of exosome vesicles were round-shaped and membrane-bounded (**Figure. 1b.**). Isolated exosomes were further characterized by particle size analyzer, which indicated exosomes as rounded particles with a diameter range 60-150nm (the average diameter of 95.5nm) in size (**Figure. 1c.**). Next, we tested whether these exosomes could be internalized by NSCs and any other surrounded cells to impact their function in the uterine or peritoneal ectopic microenvironment. Briefly, exosomes were labeled with DiR, a lipophilic fluorescent cyanine dye. DiR-labeled exosomes were then incubated with NSCs for 24h, and the internalization of these exosomes was assessed using a fluorescence microscope. It was observed that DiR-labelled exosomes were internalized into the cytoplasm of NSCs (**Figure. 1d.**). This result confirmed that exosomes derived from ESCs could be taken up and internalized by ESCs.

ESCs-derived exosomes induce NSCs migration, angiogenesis, and up-regulate inflammatory cytokines expression in ovarian cells

To identify our hypothesis that ESCs-derived exosomes can affect the NESC and the cells surrounding the ectopic lesion, exosomes isolated from ESCs were added to NESC and subjected to wound-healing and migration assay to evaluate cell motility and migration. Cells treated with exosomes-free standard culture medium were used as control. The wound-healing assay showed that ESCs-derived exosomes significantly improved the mobility of NESC, the migration rate of NESC was 18.33% compared to NESC ectopic exosomes which were 30.67% in the first 24h ($t = 3.48, p = 0.0083$). After 48h, the migration rate of NESC increased to 33.67%, while the rate of NESC ectopic exosomes was increased to 56.33% ($t = 6.39, p = 0.0002$) (**Figure. 2a.**). Transwell assay further confirmed that the ESCs-derived exosomes promoted NESC migration, in which, the number of migrated NESC was more than two times higher in the ESCs-derived exosomes group (37.59 ± 1.372) compared to the control group (14.61 ± 0.7968) ($t = 14.68, p < 0.0001$) (**Figure. 2b.**). We assessed the Epithelial-Mesenchymal Transition (EMT) related proteins, including Vimentin, N-cadherin, E-cadherin, β -catenin, Slug, Snail, ZEB1, ZO-1, and Claudin-1 by western blotting. Interestingly, the result showed that only Vimentin, β -catenin, and N-cadherin were expressed in the primary endometrial cell. Moreover, the expression of these three proteins showed no change after treated with ectopic exosome. However, the expression of MMP9, which is one of the classic MMP family proteins, was increased treated with NESC ectopic Exo (**Figure. 2c.**).

Furthermore, to evaluate the effect of ESCs-derived exosomes in angiogenesis, we conducted the tube formation assay. HUVECs were treated with the exosomes isolated from ESCs as previously described, and HUVECs were incubated in a Normal culture medium as control. We observed that HUVECs treated with ESCs-derived exosomes showed a significant increase in the number of generated loops compared to the control group ($t = 3.116, P = 0.034$), and no significant difference was noted in the loop length/per loop in two groups (**Figure. 2d.**). We further looked into the expression of several angiogenesis-related proteins in HUVECs treated with ESCs derived exosomes and normal culture media by western blotting,

using GAPDH as the internal control. The result indicated that there was no significant difference in the expression level of VEGFR2 and PDGFR, whereas the P-VEGFR2 expression level was significantly higher in HUVECs treated with ESCs-derived exosomes than in the control group. The level of P-PDGFR expression was also increased, but less than P-VEGFR2 (**Figure. 2e.**). This provided further evidence of the significant effect of ESCs-derived exosomes in regulating angiogenesis.

Moreover, endometriosis has been thought to be an inflammatory disease, and previous work showed that the expression level of pro-inflammatory cytokines was increased in peritoneal fluid. In the belief that ESCs-derived exosomes may contribute to the onset of inflammation in the ectopic lesion surrounded environment, we evaluated the gene expression level of pro-inflammatory cytokines in normal ovarian stromal cells by real-time qPCR analysis. Normal ovarian stromal cells were treated with ESCs-derived exosomes for 24h and with PBS/exosomes-free normal culture medium as control. We observed that expression levels of pro-inflammatory cytokines, including IL-1 β , IL-18, INF-1 α , TNF- α , and ICAM-1 were significantly higher in normal ovarian stromal cells treated with ESCs-derived exosomes compared to the control group ($P < 0.0001$) (Fig. 2f), indicating that ESCs-derived exosomes increased the expression of inflammatory cytokines. Taken together, these results suggested that exosomes contributed to the development of endometriosis.

Characterization of exosomal protein derived from ESCs versus NESCes by Mass Spectrometry (MS)

To characterize the protein components of NESCes and ESCes exosomes, we performed MS analysis in exosomes isolated from ESCes and NESCes supernatants. Proteomic analysis revealed a total of 155 proteins were in the cargo of exosomes from both groups, with 139 proteins were significantly expressed in ESCes exosomes (**Supplementary Table. 1**). Gene Ontology (GO) classification using Funrich function enrichment analysis [19] identified several biological processes that enriched for molecular functions (MFs), including regulation of the biological process, biological regulation, cellular process, metabolic process, and response to the stimulus (**Figure. 3a.**). To assess the differentially expressed proteins between NESCes and ESCes exosomes, we calculated two factors that constitute the fold change of protein expression and LFQ intensity between the two groups of samples, and a shuttle plot was generated (**Figure. 3b.**). A total of 6 proteins were significantly up-regulated in ESCes exosomes with criteria of $P < 0.05$, while three proteins were remarkably down-regulated in ESCes exosomes ($P < 0.05$) (**Table. 3.**). A heatmap of these up-regulated and downregulated proteins were generated to highlight the differences between NESCes and ESCes exosomes (**Figure. 3c.**). According to the KEGG pathway, we found a proteoglycan-related molecule– Moesin (MSN), which is one of the up-regulated proteins in ESCes exosomes, and is thought to be involved in angiogenesis, migration, and cell adhesion. Therefore, we evaluated the expression of moesin in exosomes from the vaginal secretion from endometriosis patients ($n = 6$) and non-endometriosis patients ($n = 10$). The result indicated that the average protein expression of MSN was 0.3217ng/ml in the control groups, which is significantly lower than in the endometriosis group (average was 0.9833) ($p = 0.0179$) (**Figure. 3d.**).

A previous study demonstrated that Estrogen (E2) regulates MSN expression by recruiting Gα₁₃ – dependent pathway to RhoA and ROCK-2[21]. Since endometriosis is thought to be closely related to high Estrogen concentration [22], thus, we aim to examine the effect of E2 on MSN expression. Treatment with E2 (10nM,50nM,100nM) induced the expression of estrogen receptor α (ERα), leading to the activation of the Gα₁₃-RhoA-ROCK-2-MSN signaling pathway, which resulted in the upregulation of MSN expression in endometriosis (**Figure. 3e.**). To test how ERα recruits the signaling of E2 to Gα₁₃ dependent pathway to regulate MSN, we silenced ERα with small interfering RNA (siRNAs). ERα expression was reduced after transfection with ERα siRNA. Western blot analysis showed that ERα silencing did not affect ERα expression, whereas RhoA, ROCK-2, MSN, and exosomal MSN expression were significantly reduced (**Figure. 3f.**), suggesting that ERα plays an important role in recruiting this signaling pathway to MSN. Nonetheless, the impact of ERα on Gα₁₃ expression needs further exploration. In addition, we have also identified the effects of other estrogen receptors, including ERβ and GPR30, in mediating the signaling of E2 to MSN (Data not shown). We observed that ERα had a significant effect on recruiting signaling of E2 to MSN (**Figure. 3g.**).

Table 3. List of 6 up-regulated proteins and 3 down-regulated proteins based on fold change in exosomes from ESCs compare to NESCs.

Protein_ID	Symbol	Entrez gene name	Sequence coverage [%]	Fold change(log2) [B/A]	P value (Significance A)
P62826	RAN	GTP-binding	23.6	2.93152	2.67E-05
E9PRK8	FTH1	Ferritin	31.6	2.06027	0.00439
J3QS39	UBB	Ubiquitin-40S ribosomal	36.6	2.03402	0.00512
V9HWC0	HEL70	Moesin	12.3	1.87496	0.01287
A0A024QYT5	SERPINE1	Serpin peptidase inhibitor, clade E member 1	34.8	1.73553	0.02842
Q16853	AOC3	Membrane primary amine oxidase [AOC3]	3.1	1.69569	0.03551

A: normal endometrial stromal cells (NESCs), B: Ectopic stromal cells (ESCs)

Exosomal Moesin promoted NESCs migration, angiogenesis, and inflammation

Through MSN siRNA transfection, we down-regulated the expression level of MSN in three primary ectopic stromal cells. The supernatant exosomes were collected, and western blot analysis showed that the exosomal MSN was significantly reduced from those three transfected ECSs (**Figure. 4a.**). To observe how exosomal MSN regulated NESCs migration, angiogenesis, and inflammation of the surrounding

tissues (ovarian epithelial cells), both ESCs exosomes and exosome^{MSNi} were co-cultured with NESC, HUVEC, and ovarian epithelial cells, respectively. Transwell assay showed that the number of NESC was notably decreased after the treatment with exosome^{MSNi} (mean \pm SD: 5.167 ± 1.169) compared to NESC + ectopic exosome group (mean \pm SD: 18.33 ± 4.274) ($t = 7.546$, $p < 0.0001$), whereas no statistical difference was observed between NESC group and NESC + ectopic exosome^{MSNi} group (**Figure. 4b.**). Simultaneously, the expression of MMP9 and EMT related proteins were detected by Western blot, the result presented that the expression of MMP9 and MSN were significantly reduced in NESC + ectopic exosome^{MSNi} group, while all the detectable EMT related proteins expression was unchanged in these three groups (**Figure. 4c.**). In the tube formation assay, lumen formation was inhibited in the NESC + ectopic exosome^{MSNi} group (**Figure. 4d.**), and expression of VEGFR2 and p-VEGFR2 were reduced (Fig. 4e). Finally, we found that mRNA expression of *IL-18*, *IL-1*, *TNF- α* , *INF- α 1*, and *ICAM1* were prominently decreased in ovarian epithelial cells treated with exosome^{MSNi} ($P < 0.0001$) (**Figure. 4f.**).

Exosome^{MSNi} inhibited the onset of intestinal heterotopic mass and peripheral inflammation in vivo

To verify the effect of exosome^{MSNi} on endometrial tissue in vivo, we divided the primary cells into 6 groups: PBS (as the control group), normal endometrial cells, ectopic endometrial cells, ectopic endometrial cells treated with MSNi, normal endometrial cells treated with exosomes derived from ectopic endometrial cells, and endometrial cells treated with exosome MSNi. We transplanted these cells into the nude mice by intraperitoneal injection. We weighed the mice every two days and found no difference between the groups (data not shown). After 10 days, we culled the mice and performed the dissection, and observed that all experiment groups of mice had heterotopic tumor growth inside the small intestine except the PBS control group. There were significant differences in the number and size of the masses formed in each group. The number and size of masses formed were increased in endometrial cells treated with ectopic exosomes group, while there was a reduction in the number and size of masses formed in the exosomal MSNi group ($P < 0.0001$) (**Figure. 5a, b.**). The number and size of masses in the ectopic groups were also notably higher than that in the normal endometrial group ($P < 0.0001$) (Fig. 5a, b), which was the same as seen in the endometrial cells treated with ectopic exosomes groups. Similarly, the intestinal mass in the ectopic group was remarkably improved after MSN down-expression ($P < 0.0001$) (**Figure. 5a, b.**). To assess the extent of peripheral inflammation, we selected the small intestine tissues with 5cm of the tumor and analyzed the expression of inflammatory factors. We observed that both ectopic endometrial cells and the normal endometrial cells treated with ectopic exosomes increased the expression of IL-18, IL-1 β , TNF- α , and adhesion factor ICAM-1, however, the knockdown of MSN reversed this change (**Figure. 5c.**).

Exosome^{MSNi} decreased the expression of MMP9 in masses and the formation of the vascular lumen in vivo

To probe into the small intestine ectopic internal MMP9 expression and angiogenesis of tumor, we performed immunohistochemistry (IHC) and immunofluorescence (IF) staining on the mass organization.

IHC staining showed that MMP9 presented more significant expression on the edge of the ectopic mass in the ectopic and normal endometrial cells treated with ectopic exosomes. In contrast, in MSN knockdown groups, the expression of MMP9 was notably decreased, whereas there was no difference in normal endometrium (**Figure. 6a.**). Meanwhile, large vascular lumens were formed in the tissue, and VEGFR2 was expressed mainly in lumens in both the ectopic group and endometrial cells treated with ectopic exosomes group. Although VEGFR2 was also expressed in the ectopic endometrial MSNi group and normal endometrial cells treated with exosome^{MSNi}, most of the lumens where VEGFR2 was expressed were narrow and partially closed (**Figure. 6b.**). We detected the expression of p-VEGFR2 in heterotopic tissue by IF staining. Similarly, we found that p-VEGFR2 was predominantly expressed in the vascular cavity in ESCs group and NESCs treated with the ectopic exosomes group, while p-VEGFR2 was only sporadically expressed in other groups (**Figure. 6c.**).

Discussion

Endometriosis has been regarded as the reflux of endometrial tissue into the peritoneal cavity by traveling through the Fallopian tubes during menstruation, where it attaches, forms an implant, and proliferate at the ectopic site [23]. While the endometrium with abnormal migration ability is the fundamental contributor to the formation of an endometriotic lesion in the ectopic area, whether the microenvironment of the ectopic implantation is conducive to adhesion and colonization of the forthcoming endometrial cells is also a critical factor. Sun et al., (2019) reported that eutopic endometrial cells-derived exosomes promote neuro-angiogenesis in endometriosis [24]. In this study, we explored the effect of exosomes derived from the ectopic endometrial cells on the progression of endometriotic lesions. We studied how the ectopic endometrium utilized exosomes to build up a “migration-inflammation-vascularisation” loop to facilitate the development of the disease.

Exosomes are small membrane vesicles that range in size, between 30–120 nm, and are released by the vast majority of cell types. It has been reported to be detectable in different kinds of body fluids, including blood, saliva, urine, and uterine fluid[25, 26]. Ouattara LA carried out an exosomal study about vaginitis, in which exosomes were extracted from patients’ vaginal secretion for follow-up detection [27]. In the current study, we isolated exosomes from ESCs and NESCs, and subjected them to Mass Spectrometry analysis (3cases, lost 1case). We found that a total of six proteins were highly expressed in ESCs exosomes, and three proteins were expressed at a relatively lower level. After analysis, we found that Moesin (MSN) showed a strong correlation with migration, angiogenesis, and inflammation. Besides, MSN was found to crosstalk the heparan sulfate proteoglycans (HSPGs) pathway with MMP9 through KEGG analysis. Interestingly, MMP9 is associated with cell migration, vascular formation, and inflammation as well [28] [29] [30].

MSN is a member of the ERM (ezrin, radixin, and moesin)protein family discovered in 1992, and other members of ERM protein include ezrin, radixin, and merlin[31]. ERM proteins are bridge molecules that cross-link the cortical actin cytoskeleton with the integrin on the plasma membrane. By mediating the connection between the cytoplasmic membrane and actin cytoskeleton, ERM proteins play a critical role

in cell growth, movement, migration, mitosis, and signal transduction[32]. In gynaecological oncology, high expression of ERM is known to promote the proliferation and migration of tumor cells, and even facilitate the formation of the blood vessel. Z Chen et al reported that activation of ezrin was increased in ovarian epithelial carcinoma (OVCA), and related to OVCA metastatic process [33]. Paulette M. et al showed that high expression of MSN in endometrial adenocarcinoma is associated with grade and subtype[34]. In this study, we identified the role of exosomes derived from ESCs, specifically of exosomal MSN, on the migration and vascularisation of normal endometrium *in vivo* and *in vitro* experiments. We observed that high expression of MSN in ectopic endometrial cells and exosomes is regulated by ER α recruiting E2 signaling to the RhoA-Rock2-MSN pathway. It is intriguing to find that the knockdown of ER α did not affect the expression of G α_{13} , although a significant reduction was observed in downstream proteins expression. This might be explained by the fact that ER α and G α_{13} work synergistically in regulating this signaling pathway. Yet, further study will be conducted to get a full understanding underlying this phenomenon.

Our results demonstrated that exosomal MSN in ESCs can improve the migration ability of the normal endometrium, as well as the number of the vascular lumen (lumen size did not change significantly vs. control group in vitro experiment). Meanwhile, the expression of inflammatory cytokines around the surrounding tissues of heterotopic foci was also up-regulated. As a consequence, the adhesion of the ectopic region was increased, which is consistent with the results from previous studies [35] [36] [37]. The KEGG pathway and western blot analysis suggested that this biological phenomenon might be related to the up-regulation of MMP9 expression by MSN.

MMP9 is a member of the MMPs family, which is a protein family of zinc-dependent endopeptidases whose primary function is to degrade the extracellular matrix (ECM) and maintain the dynamic balance of the extracellular matrix. MMP9 involves tissue remodeling, organogenesis, inflammation, initiation of cancer, as well as other physiological and pathological processes[38, 39]. Numerous studies have shown that the high expression of MMP9 is associated with the improvement of tumor migration and invasion ability [40] [41] [42]. In this study, the increase in normal endometrial migration was achieved by the up-regulation of MMP9 expression by ectopic exosomes, which was reversed by MSNi exosomes. Meanwhile, angiogenesis and the expression of inflammatory factors in surrounding tissues induced by ectopic exosomes might also be correlated with the overexpression of MMP9. There is a study on the correlation between MSN and MMP9 showed that, in individual tumors, the expression of MSN and MMP9 remains consistent, which jointly promotes tumor metastasis [43]. In our study, ectopic exosomal MSN up-regulated the expression of MMP9 in target cells and induced an increase in the secretion of VEGF, thereby promoting angiogenesis. This suggests that endometriosis shares similar characteristics with tumors in certain aspects. However, it should be taken into consideration that the migration of normal endometrial cells is not the result of EMT, as it is mostly the case in cancer. Therefore, the ability of migration and invasion of the ectopic cells is significantly weaker than that of the cancer cells.

There are not many studies that provide evidence for the correlation between MSN and inflammatory factors. Nevertheless, it has been reported that the expression of MSN might be related to the recruitment

of neutrophils. In the current study, the reduction in the expression of inflammatory factors caused by the knockdown of exosomal MSN might still be associated with the inhibition of MMP9 expression in cells. The relevant evidence will be verified continually in subsequent experiments. Besides, we found that exosomal moesin deficiency can suppress the size of the ectopic foci. However, in the in-vitro experiment, ectopic exosomes not significantly increased the proliferation of normal endometrium (data are not shown). Thus, we supposed that increase migration and angiogenesis caused the differences in the size of heterotopic foci.

Conclusion

In conclusion, by distal secretion manner, ESCs at the site of ectopic lesions utilized exosomes to transfer MSN to NESCs, thereby impact the migration ability of normal endometrium. Meanwhile, we noticed that an abnormal estrogen concentration may partly contribute to the high expression of MSN in exosomes derived from ESCs. Furthermore, exosomal MSN induced the high expression of inflammatory cytokines in surrounding tissue of ectopic lesions, leading to the increase in cell adhesion and angiogenesis in surrounding ectopic tissue. Finally, the construction of a “migration-inflammation-vascularisation” loop connecting normal endometrium and ectopic endometrium facilitated the progression of endometriosis. Overall, our study suggested that exosome, with its important biological function as a carrier of genetic information between cells, could contribute to the development of EMS. Future exploration should be made to further understand the mechanism driving the aberrant expression of exosomal composition, as well as developing therapies targeting exosomal composition that can decrease ectopic implantation of endometrial tissue.

Declarations

Ethics approval and consent to participate

All animal experiments were performed under the approval of the committee on the Ethical Use of Animals of Medical School of Ningbo University and under the Guide for the Care and Use of Laboratory animals. All patients sample were collected after the written informed consent was obtained, and all procedures were approved by the ethical committee of the Affiliated Hospital of Ningbo Medical School of Ningbo University.

Consent for publication

Not applicable

Availability of supporting data

The dataset generated and/or analyzed during the current study is all included in this paper.

Competing interests

All authors stated that they have no conflict of interests.

Funding

This work is supported by a Project supported by the National Science Foundation for Young Scientists of China (Grant No. 81901459), Public Welfare Projects in Zhejiang Province (Grant No. LGF19H040003) Natural Science Foundation of Zhejiang Province (Grant No. LH18Y040009), Ningbo Natural Science Foundation (Grant No.2017A610161)

Authors' contribution

YC-C and MA: Designed the study, conducted experiments, analyzed the data, performed the statistical analysis, and wrote the manuscript. XD-F, J-Z: Conducted experiments, analyzed the data. JJ-L: Provided scientific support and discussion. XM-Z: Critically reviewed the manuscript and provided scientific support for experiments. All authors read and approved the final version of the manuscript.

Corresponding author

Correspondence to [Yichen Chen](#).

Acknowledgments

Not applicable

References

1. Miller, J.E., et al., *Implications of immune dysfunction on endometriosis associated infertility*. *Oncotarget*, 2017. **8**(4): p. 7138-7147.
2. Culley, L., et al., *The social and psychological impact of endometriosis on women's lives: a critical narrative review*. *Hum Reprod Update*, 2013. **19**(6): p. 625-39.
3. Cramer, D.W. and S.A. Missmer, *The epidemiology of endometriosis*. *Ann N Y Acad Sci*, 2002. **955**: p. 11-22; discussion 34-6, 396-406.
4. Sasson, I.E. and H.S. Taylor, *Stem cells and the pathogenesis of endometriosis*. *Ann N Y Acad Sci*, 2008. **1127**: p. 106-15.
5. Filippi, I., et al., *Different Expression of Hypoxic and Angiogenic Factors in Human Endometriotic Lesions*. *Reprod Sci*, 2016. **23**(4): p. 492-7.
6. Guo, S.W., Y. Du, and X. Liu, *Endometriosis-Derived Stromal Cells Secrete Thrombin and Thromboxane A2, Inducing Platelet Activation*. *Reprod Sci*, 2016. **23**(8): p. 1044-52.

7. Rocha, A.L., F.M. Reis, and R.N. Taylor, *Angiogenesis and endometriosis*. *Obstet Gynecol Int*, 2013. **2013**: p. 859619.
8. Gazvani, R. and A. Templeton, *Peritoneal environment, cytokines and angiogenesis in the pathophysiology of endometriosis*. *Reproduction*, 2002. **123**(2): p. 217-26.
9. Laschke, M.W. and M.D. Menger, *In vitro and in vivo approaches to study angiogenesis in the pathophysiology and therapy of endometriosis*. *Hum Reprod Update*, 2007. **13**(4): p. 331-42.
10. Ahn, S.H., et al., *IL-17A Contributes to the Pathogenesis of Endometriosis by Triggering Proinflammatory Cytokines and Angiogenic Growth Factors*. *J Immunol*, 2015. **195**(6): p. 2591-600.
11. Khalaj, K., et al., *A balancing act: RNA binding protein HuR/TTP axis in endometriosis patients*. *Sci Rep*, 2017. **7**(1): p. 5883.
12. Ge, R., et al., *Exosomes in Cancer Microenvironment and Beyond: have we Overlooked these Extracellular Messengers?* *Cancer Microenviron*, 2012. **5**(3): p. 323-32.
13. Zhu, Q., et al., *Microfluidic engineering of exosomes: editing cellular messages for precision therapeutics*. *Lab Chip*, 2018. **18**(12): p. 1690-1703.
14. Azmi, A.S., B. Bao, and F.H. Sarkar, *Exosomes in cancer development, metastasis, and drug resistance: a comprehensive review*. *Cancer Metastasis Rev*, 2013. **32**(3-4): p. 623-42.
15. De Toro, J., et al., *Emerging roles of exosomes in normal and pathological conditions: new insights for diagnosis and therapeutic applications*. *Front Immunol*, 2015. **6**: p. 203.
16. Zhang, A., et al., *Exosome-mediated microRNA-138 and vascular endothelial growth factor in endometriosis through inflammation and apoptosis via the nuclear factor-kappaB signaling pathway*. *Int J Mol Med*, 2019. **43**(1): p. 358-370.
17. Wu, D., et al., *Exosomal miR-214 from endometrial stromal cells inhibits endometriosis fibrosis*. *Mol Hum Reprod*, 2018. **24**(7): p. 357-365.
18. Harp, D., et al., *Exosomes derived from endometriotic stromal cells have enhanced angiogenic effects in vitro*. *Cell Tissue Res*, 2016. **365**(1): p. 187-96.
19. Lasser, C., M. Eldh, and J. Lotvall, *Isolation and characterization of RNA-containing exosomes*. *J Vis Exp*, 2012(59): p. e3037.
20. Gotz, S., et al., *High-throughput functional annotation and data mining with the Blast2GO suite*. *Nucleic Acids Res*, 2008. **36**(10): p. 3420-35.
21. Sanchez, A.M., et al., *Rapid signaling of estrogen to WAVE1 and moesin controls neuronal spine formation via the actin cytoskeleton*. *Mol Endocrinol*, 2009. **23**(8): p. 1193-202.

22. Othman, E.R., et al., *Markers of Local and Systemic Estrogen Metabolism in Endometriosis*. *Reprod Sci*, 2020.
23. Simpson, J.L., et al., *Genetics of endometriosis*. *Obstet Gynecol Clin North Am*, 2003. **30**(1): p. 21-40, vii.
24. Sun, H., et al., *Eutopic stromal cells of endometriosis promote neuroangiogenesis via exosome pathway*. *Biol Reprod*, 2019. **100**(3): p. 649-659.
25. Vlassov, A.V., et al., *Exosomes: current knowledge of their composition, biological functions, and diagnostic and therapeutic potentials*. *Biochim Biophys Acta*, 2012. **1820**(7): p. 940-8.
26. Burns, G., et al., *Extracellular vesicles in luminal fluid of the ovine uterus*. *PLoS One*, 2014. **9**(3): p. e90913.
27. Ouattara, L.A., S.M. Anderson, and G.F. Doncel, *Seminal exosomes and HIV-1 transmission*. *Andrologia*, 2018. **50**(11): p. e13220.
28. Liu, H., et al., *GLI1 is increased in ovarian endometriosis and regulates migration, invasion and proliferation of human endometrial stromal cells in endometriosis*. *Ann Transl Med*, 2019. **7**(22): p. 663.
29. Li, L., et al., *Herbacetin suppressed MMP9 mediated angiogenesis of malignant melanoma through blocking EGFR-ERK/AKT signaling pathway*. *Biochimie*, 2019. **162**: p. 198-207.
30. Hernandez, P., et al., *Severe Burn-Induced Inflammation and Remodeling of Achilles Tendon in a Rat Model*. *Shock*, 2018. **50**(3): p. 346-350.
31. Ivetic, A. and A.J. Ridley, *Ezrin/radixin/moesin proteins and Rho GTPase signalling in leucocytes*. *Immunology*, 2004. **112**(2): p. 165-76.
32. Polesello, C. and F. Payre, *Small is beautiful: what flies tell us about ERM protein function in development*. *Trends Cell Biol*, 2004. **14**(6): p. 294-302.
33. Chen, Z., et al., *Ovarian epithelial carcinoma tyrosine phosphorylation, cell proliferation, and ezrin translocation are stimulated by interleukin 1alpha and epidermal growth factor*. *Cancer*, 2001. **92**(12): p. 3068-75.
34. Mhaweche-Fauceglia, P., et al., *Claudin7 and moesin in endometrial Adenocarcinoma; a retrospective study of 265 patients*. *BMC Res Notes*, 2012. **5**: p. 65.
35. Bedir, R., et al., *The role of the adhesion molecule Nectin-4 in the pathogenesis of endometriosis*. *Clin Exp Obstet Gynecol*, 2016. **43**(3): p. 463-6.
36. Liu, D., et al., *Increased expression of epithelial cell adhesion molecule and its possible role in epithelial-mesenchymal transition in endometriosis*. *J Obstet Gynaecol Res*, 2020. **46**(10): p. 2066-2075.

37. Lee, Y., et al., *Correlation of preoperative biomarkers with severity of adhesion in endometriosis*. J Gynecol Obstet Hum Reprod, 2020. **49**(1): p. 101637.
38. Back, M., D.F. Ketelhuth, and S. Agewall, *Matrix metalloproteinases in atherothrombosis*. Prog Cardiovasc Dis, 2010. **52**(5): p. 410-28.
39. Li, X. and J.F. Wu, *Recent developments in patent anti-cancer agents targeting the matrix metalloproteinases (MMPs)*. Recent Pat Anticancer Drug Discov, 2010. **5**(2): p. 109-41.
40. Chen, Y.S., et al., *HSP40 co-chaperone protein Tid1 suppresses metastasis of head and neck cancer by inhibiting Galectin-7-TCF3-MMP9 axis signaling*. Theranostics, 2018. **8**(14): p. 3841-3855.
41. Li, W., et al., *Golgi phosphoprotein 3 regulates metastasis of prostate cancer via matrix metalloproteinase 9*. Int J Clin Exp Pathol, 2015. **8**(4): p. 3691-700.
42. Guo, J., et al., *Effects of exposure to benzo[a]pyrene on metastasis of breast cancer are mediated through ROS-ERK-MMP9 axis signaling*. Toxicol Lett, 2015. **234**(3): p. 201-10.
43. Lan, S., et al., *Moesin facilitates metastasis of hepatocellular carcinoma cells by improving invadopodia formation and activating beta-catenin/MMP9 axis*. Biochem Biophys Res Commun, 2020. **524**(4): p. 861-868.

Figures

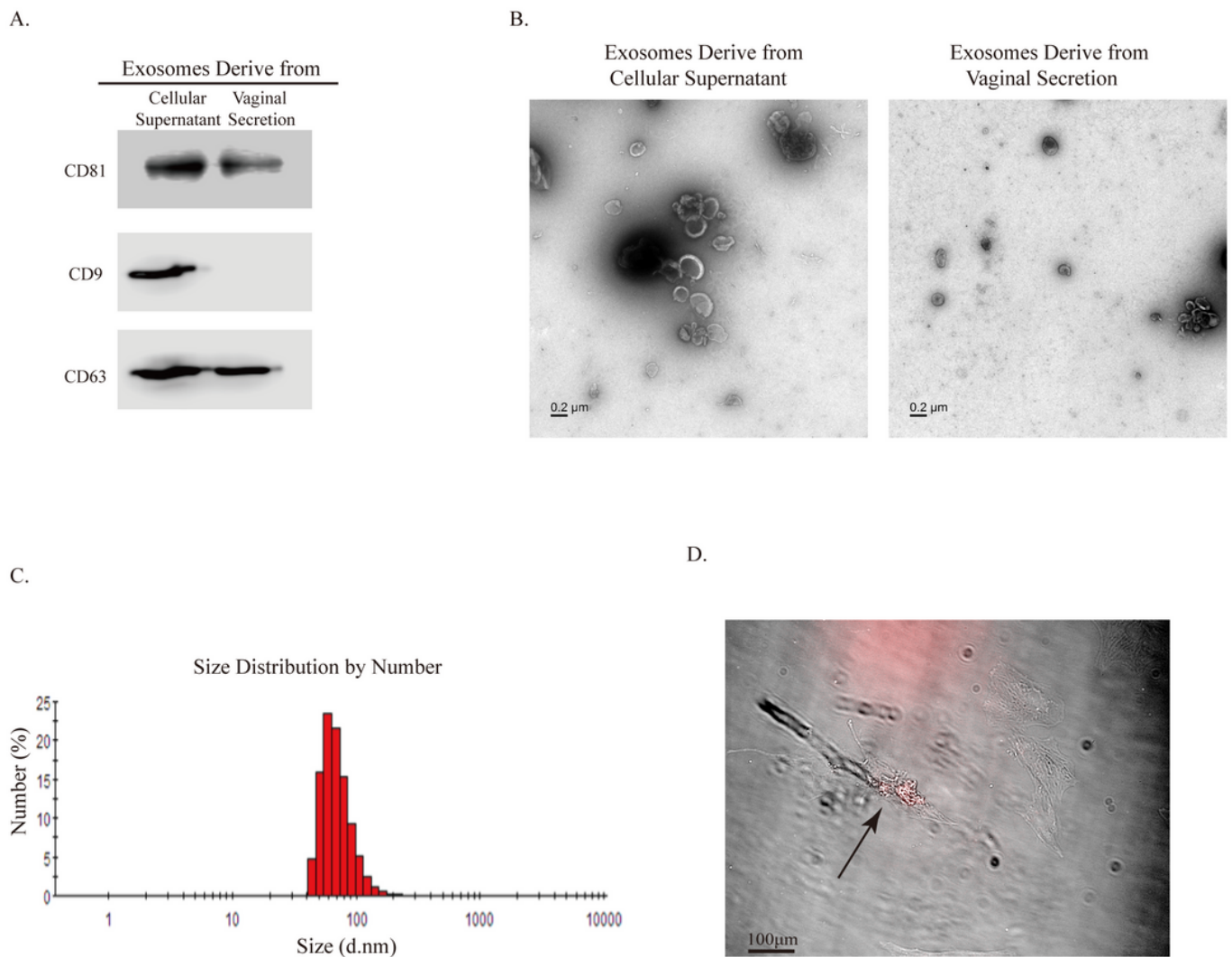


Figure 1

a: Western blot analysis of exosomal marker CD63, CD81, and CD9 in exosomes from primary cellular supernatant and vaginal secretion. CD9 did not express in exosomes derived from vaginal secretion. b: Transmission electron microscope (TEM) of exosomes. c: The average size of exosomes is 95.5nm. d: DiR staining of exosomes into Normal endometrial stromal cells (NESC) was observed by the fluorescence microscope (200x).

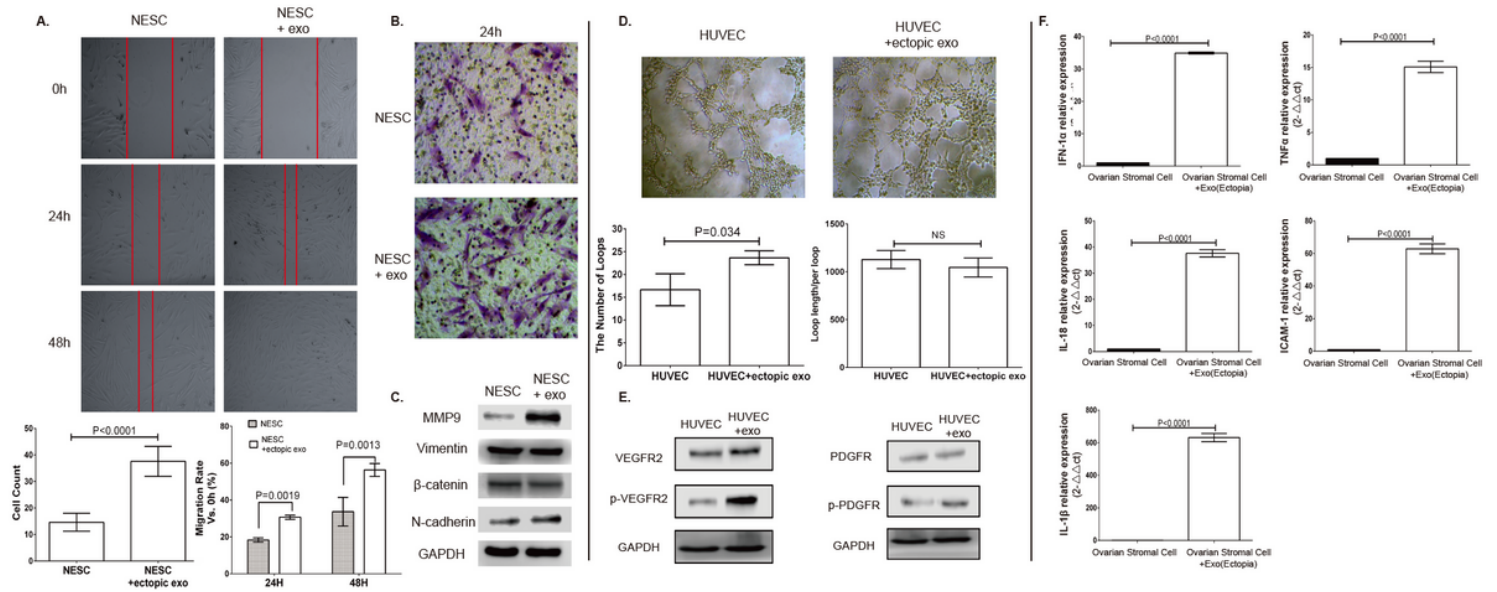


Figure 2

a: Wound-healing assay to verify the effects of exosomes on normal endometrial stromal cells (NESC) migration. b. Transwell assay to evaluate the migration ability, along with the quantification of migrated cells and migration rate. c. Western blotting showed ectopic exosomes overexpressed MMP9, but there were no changes in the expression level of EMT-related proteins. d. A tube formation assay along with quantification of the number of loops formed and loop length/per loop. e. Western blotting analysis assessed the expression of VEGFR2 and P-VEGFR2. f. qRT-PCR tested the expression of inflammatory cytokines: IL-1 β , IL-18, INF-1 α , TNF- α and ICAM-1, ectopic exosomes up-regulated those inflammatory cytokines. Data were expressed as mean \pm SEM, NS, no significance, **** $P < 0.0001$.

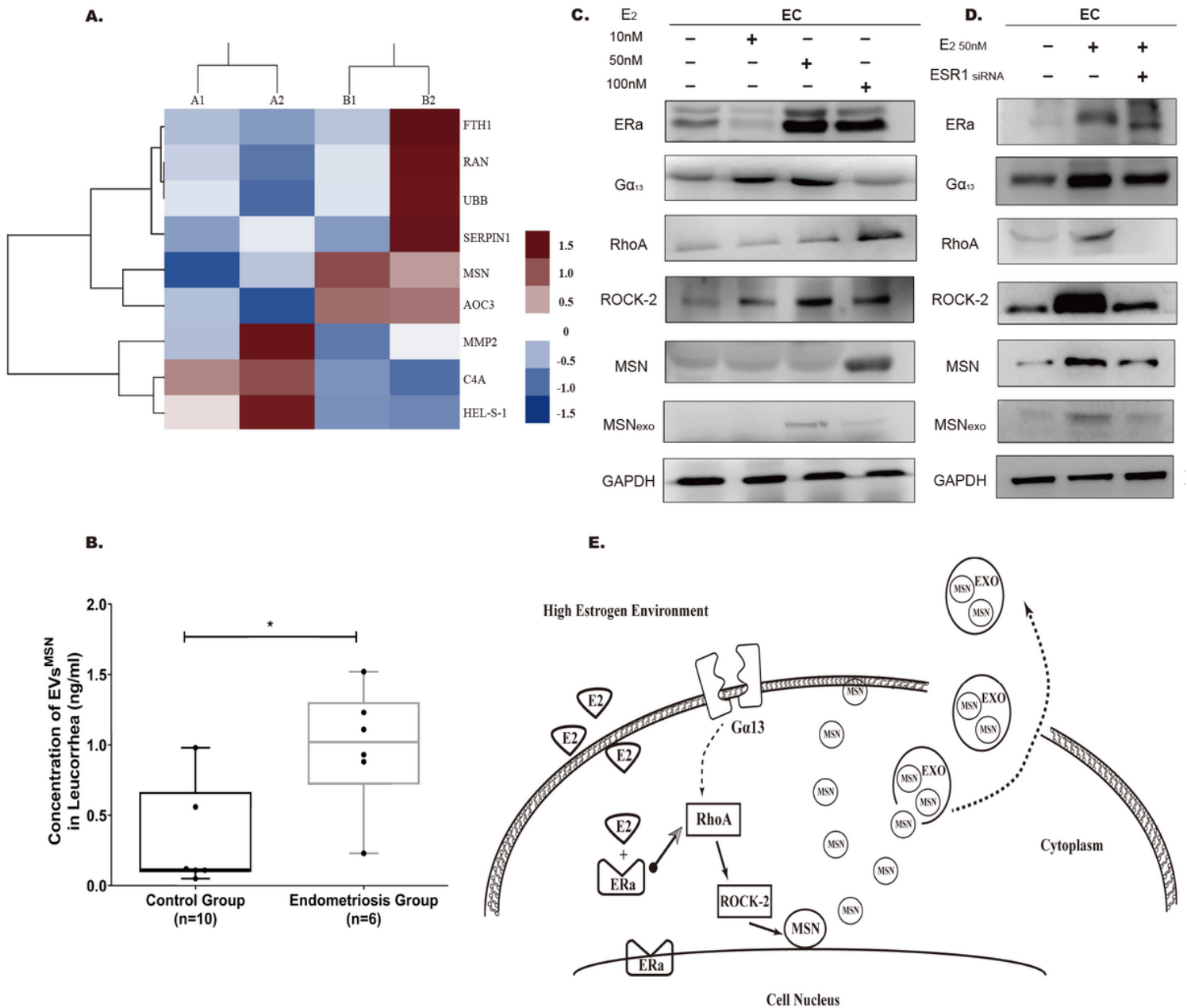


Figure 3

The proteome profile of NESCs- and ESCs exosomes. a. Total of 155 proteins was identified by mass spectrometry. All identified proteins were submitted to the GO classification system using Funrich analysis. b. shuttle plot of the proteomic data between NESCs and ESCs exosomes. Y-axis of the plot represents significance ($-\log_{10}$ of p-value), and the x-axis shows the \log_2 of the fold-change (ESCs(B)/NESCs (A) exosomes). The fold changes of proteins not statistically significant are represented as blue dots, the red dots are represented 0.01

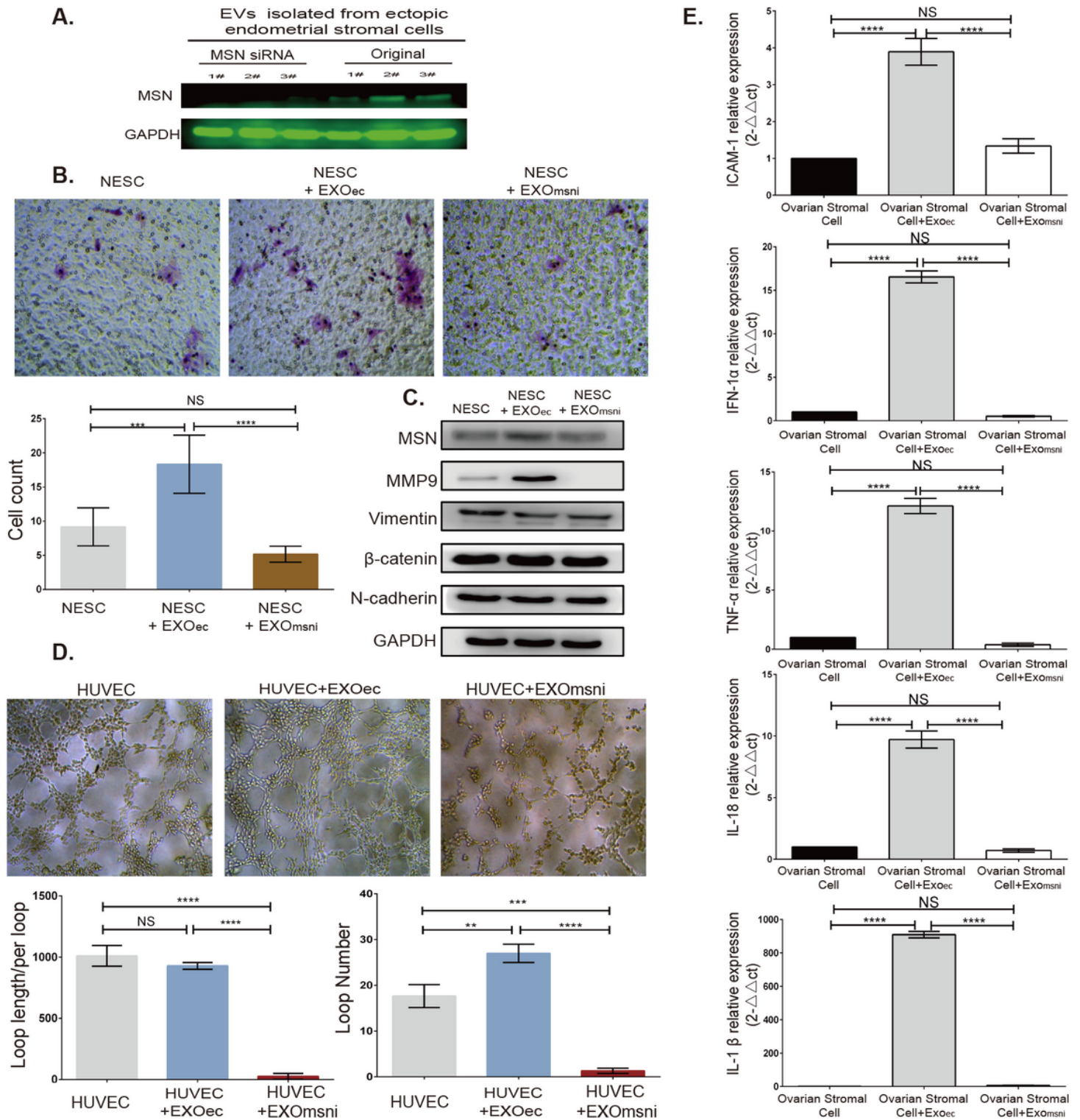
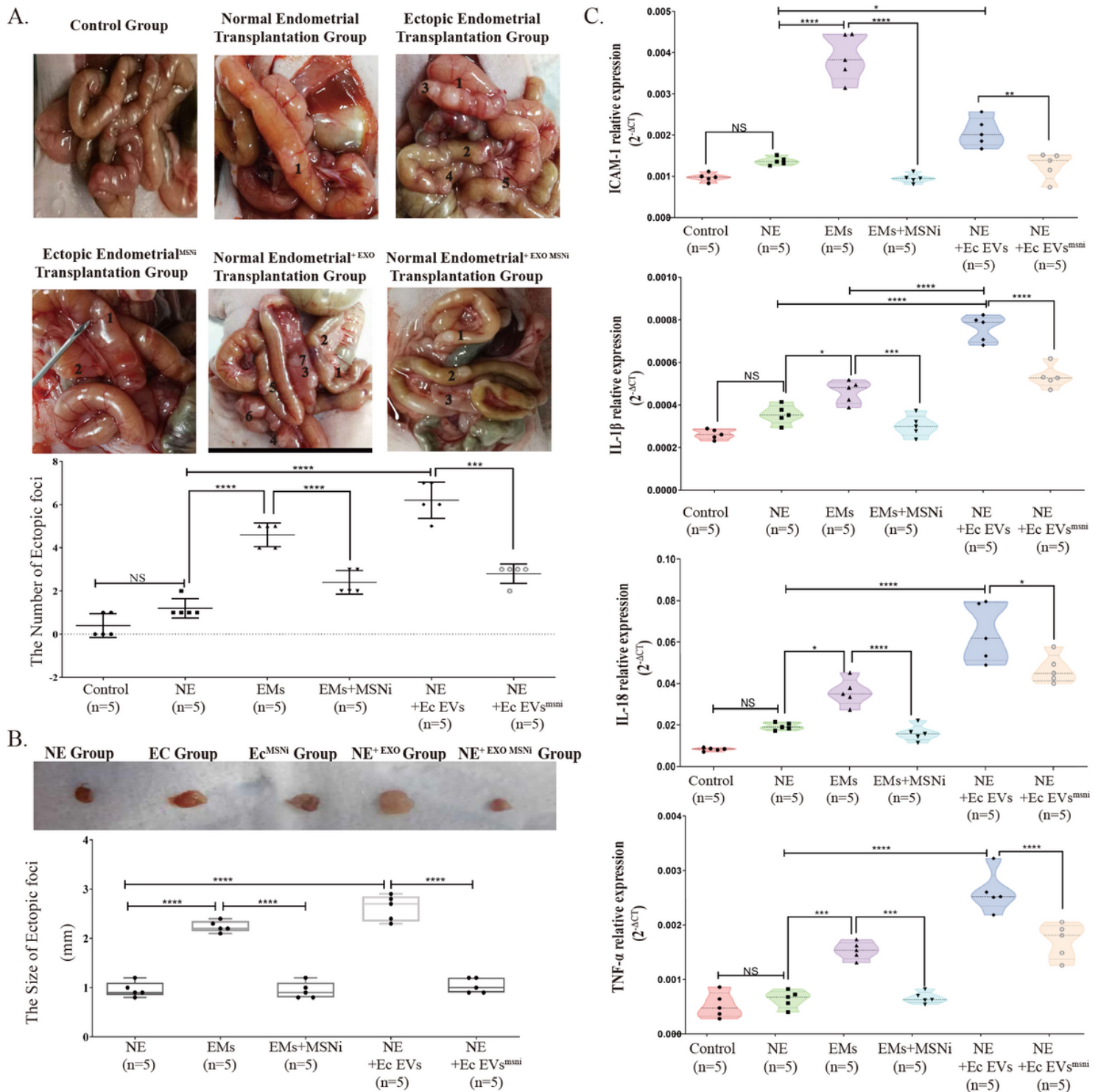
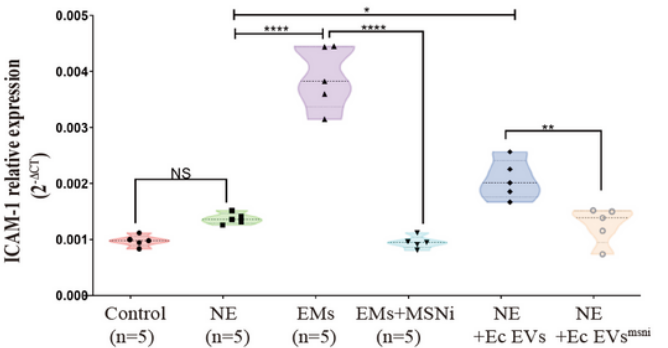


Figure 4

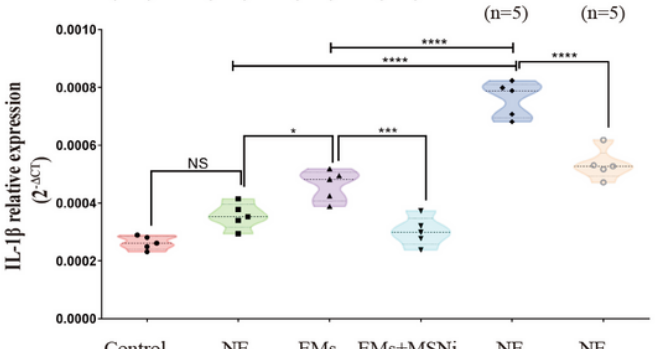
a. The expression of exosomal MSN. b. Transwell assay evaluated the migration of N ESCs treated with exosome+MSN. c. Western blot qualified the expression of MSN, MMP9, and EMT-related proteins. d. A tube formation after exo+MSN treatment. e. WB tested the expression of VEGFR2 and p-VEGFR2. f. qRT-PCR. Data were expressed as mean \pm SEM, NS, no significance, **** P<0.0001.



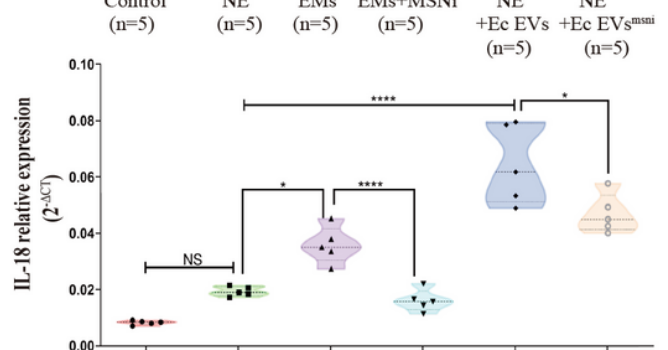
ICAM-1 relative expression (2^{-ΔCT})



IL-1β relative expression (2^{-ΔCT})



IL-18 relative expression (2^{-ΔCT})



TNF-α relative expression (2^{-ΔCT})

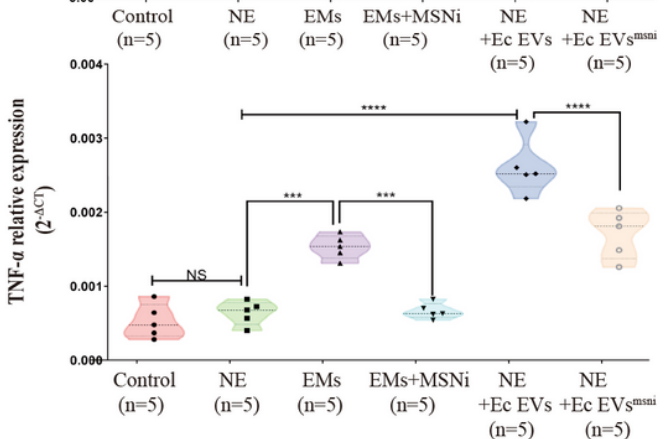


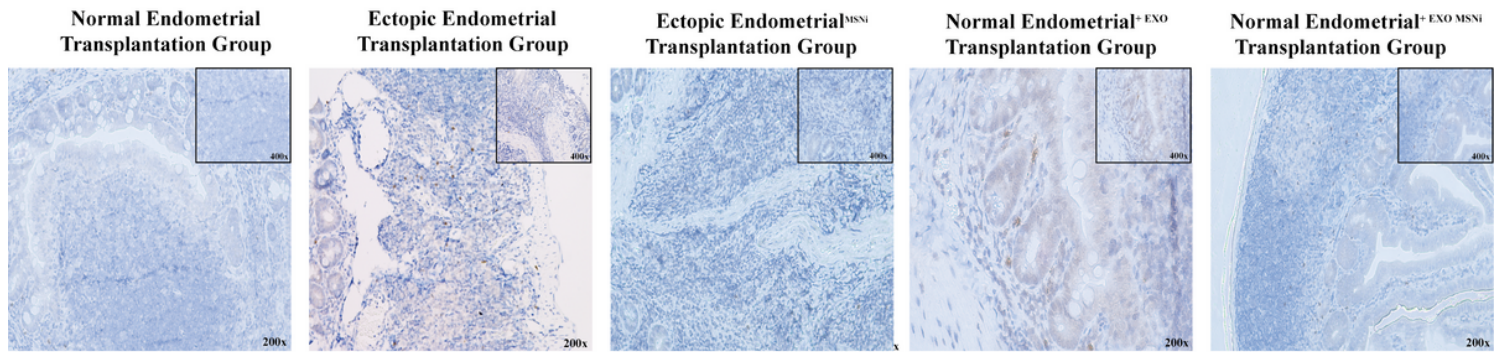
Figure 5

a: The model of heterotopia mouse was constructed by intraperitoneal injection. Ectopic stromal cells and normal endometrial stromal cells+ectopic exosomes notably increased the number of ectopic foci compared with the normal endometrial stromal cells group and control group ($p < 0.0001$), while MSNi and exosomal MSNi inhibited this phenomenon ($P < 0.0005$). b: The size of ectopic implant tissue. Ectopic exosomes could increase the size of ectopic tissue the same as the ectopic cells, but exosomal MSNi and ectopic cells+MSNi decreased the size ($P < 0.0001$). c: The expression of inflammatory cytokines: IL-1β,

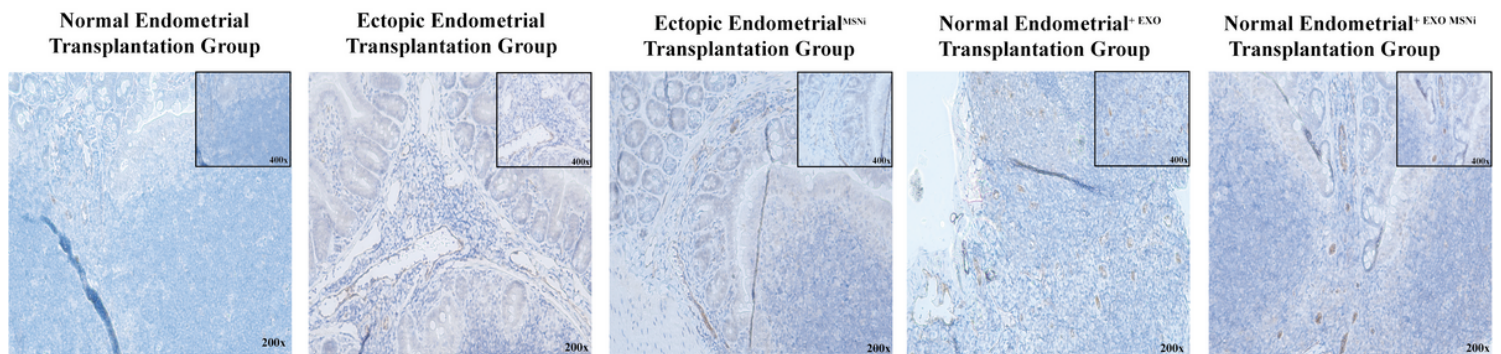
ICAM-1, IL-18, and TNF- α in the small intestinal tissue surrounding the heterotopic foci. Data were expressed as mean \pm SEM, NS, no significance, **** P<0.0001.

A.

The Expression of MMP9 in vivo



B.
The Expression of VEGFR2 in vivo



C.
The Expression of p-VEGFR2 in vivo

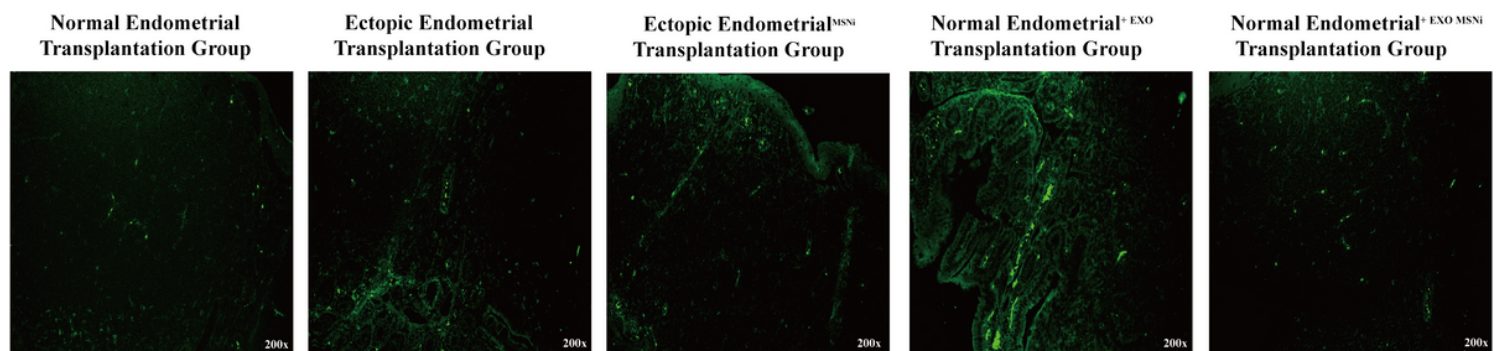


Figure 6

a. MMP9 expressed in ectopic implant tissues detected by Immunohistochemistry. b. VEGFR2 expressed in ectopic implant tissues detected by Immunohistochemistry. c. Immunofluorescence of p-VEGFR2 in ectopic foci. The result was consistent with VEGFR2. MSNi: MSN siRNA transfection; Microscopic magnification: 200x.

Supplementary Files

This is a list of supplementary files associated with this preprint. Click to download.

- [supplementaryTable.xlsx](#)